

Article

The Effectiveness of Swiveling Seats in Protecting Reclined Occupants in Highly Autonomous Driving Environments during Frontal Crashes

Fang Tong ^{1,2,*}, Yuchao Wang ¹, Qifei Jian ², Fengchong Lan ² and Jiqing Chen ²¹ GAC Automotive Research & Development Center, Guangzhou 511434, China; wangyc@gacrnd.com² School of Mechanical & Automotive Engineering, South China University of Technology, Guangzhou 510641, China; tcjqf@scut.edu.cn (Q.J.); fclan@scut.edu.cn (F.L.); chjq@scut.edu.cn (J.C.)

* Correspondence: tongfang@gacrnd.com

Abstract: High-tilt reclined seats are one of the most popular configurations in highly automated vehicles; however, current restraint systems cannot protect out-of-position occupants in this type of seat. To reduce the risk of injury to reclined occupants, this study proposes a swiveling seat driven by occupant inertia and rotated in the sagittal plane during impact. The effectiveness of the swiveling seat was evaluated based on kinematics and injury to a human biomechanical model in a frontal sled test. A simulation matrix was constructed to design and optimize various safety devices, including the belt, pre-tensioner, knee constraint, and rotation stiffness for the swiveling seat. The results showed that (1) submarining occurred when the reclined occupant was on a fixed seat with a normal three-point belt during impact; (2) a fixed seat with a dynamic locking tongue and passenger lap pretension prevented the submarining, but produced a high lumbar force of 5359 N, which was higher than the spine injury criterion; and (3) the proposed swiveling seat with a matched restraint system could prevent submarining and produce lumbar force of 1787 N. The results demonstrated that the swiveling seat has high potential for occupant protection in intelligent driving scenarios.

Keywords: reclined occupant; swiveling seat; impact response; submarining; lumbar force



Citation: Tong, F.; Wang, Y.; Jian, Q.; Lan, F.; Chen, J. The Effectiveness of Swiveling Seats in Protecting Reclined Occupants in Highly Autonomous Driving Environments during Frontal Crashes. *Appl. Sci.* **2024**, *14*, 349. <https://doi.org/10.3390/app14010349>

Academic Editors: Arkady Voloshin and Heecheon You

Received: 7 November 2023

Revised: 22 December 2023

Accepted: 26 December 2023

Published: 29 December 2023



Copyright: © 2023 by the authors. Licensee MDPI, Basel, Switzerland. This article is an open access article distributed under the terms and conditions of the Creative Commons Attribution (CC BY) license (<https://creativecommons.org/licenses/by/4.0/>).

1. Introduction

Automobile manufacturers are increasingly using high-tilt-back seats to improve passenger comfort. The development of highly automated vehicles may introduce occupants with new seating positions and configurations, among which reclined seating is one of the most popular [1–3]. Ostling et al. [4] investigated how 149 participants from China and Sweden wished to sit via the “Setting the stage” method. The results showed that comfortable and reclined seats were frequently mentioned, and that participants could accept extra restraints to maintain their current safety level if more sitting postures were available [5]. However, traditional restraint systems, such as three-point seat belts and airbags mounted on the steering wheels were unsatisfactory in protecting reclined passengers, and even caused serious injuries to passengers, including strangulation across the neck [6,7]. Therefore, there is a growing need to develop novel safety systems to match reclined sitting postures.

Several studies have investigated reclined occupant injuries in autonomous driving vehicles based on numerical studies and post-mortem human subjects (PMHS) experiments [8–12]. The key challenge in protecting the reclined occupants is to balance the problem of submarining with the high lumbar load associated with anti-submarining devices. Frontal impact simulations using the Global Human Body Model Consortium (GHBMC) occupant model showed that a higher pelvic angle resulted in higher risk of submarining [13]. Rawska et al. [14] adopted a knee bolster to prevent submarining and observed an increased lumbar flexion load in a human model. The PMHS experiments conducted by

Richardson et al. [15,16] also showed that the lumbar spine is subjected to high bending and compression in a reclined posture, owing to the movement of the upper torso.

Several safety devices have been proposed for the reclining occupant. Matsushita et al. [17] designed a dual shoulder airbag (DSA) system that could be deployed from both sides of the seatback and seat pan to raise the occupant's pelvis and thigh area to avoid submarining. The study illustrated the effectiveness of the DSA based on head, neck, and chest injuries of the Hybrid III and THOR dummies, whereas the lumbar spine, with a high potential risk of injury, was not evaluated. Rawska et al. [18] predicted that submarining was the major challenge for reclined occupants, and adopted a knee bolster to restrain the forward movement of the passenger's knee and reduce submarine risk. A high lumbar force was discovered in the 30° seatback sled simulation; however, no countermeasures were proposed. Although these methods protect the reclined occupant in situ, high spinal force remains unresolved. Some car manufacturers protect reclined occupants by adjusting the seatback angle to maintain normal posture before a crash [19]. However, in this proactive safety seat, the rotation speed of the seatback was restricted to <10°/s because of the maximum allowed voltage capacity of the battery, costing 3–5 s to upright the seatback. This means that the car should detect the crash 3–5 s in advance and transmit the signal to the seat to adjust the backrest, which brings a high requirement for predicting the collision risk.

The current study proposed a swiveling seat in which reclined occupants could move upright using their own inertia during frontal impact. Additionally, related constrained systems for the swiveling seat, such as the belt position and force limit, dynamic locking tongue (DLT), and passenger lap pretension (PLP), were further investigated using a simulation matrix. The crash configuration was derived from the sled test of a full frontal rigid barrier at 50 km/h. Injury indices of the head, thorax, abdomen, pelvis, and lower limbs of the occupants were used to evaluate the effectiveness of the swiveling seat.

2. Materials and Methods

2.1. Models

Human biomechanical models perform better than dummy models in studying passengers injuries in out-of-seat position, particularly in reclined postures. Because dummies such as THOR and WorldSID were designed for the assessment of occupant injury with a standard sitting posture, the stiffness of the lumbar spine in dummies makes it difficult to position the dummy in a natural lying configuration. Subsequently, the 50th percentile THUMS V6 model was simulated. THUMS is a biomechanical model that depicts the human skeleton, muscles, and organs based on the finite element method, as shown in Figure 1. The model consists of the head, neck, torso, and upper and lower limbs. The most vulnerable parts of the reclined occupants of the abdomen, pelvis, and spine were also modeled in detail according to human anatomy. The element length of the THUMS was 3–5 mm, and the reference values for the quality of the element geometry were set as follows: warpage, 50° or less; aspect ratio, 5° or less; skew, 60° or less; and Jacobian, 0.3 or more. The skeletal parts of the THUMS were assumed to have elastoplastic properties, and a hyperelastic material was assumed for the soft tissues. The impact responses of the THUMS were verified by simulating 38 cadaver impact tests described in the literature (refer to the Documentation of Total Human Model for Safety (THUMS) <https://www.toyota.co.jp/thums/>, accessed on 25 December 2023).

The original posture of the THUMS was the driving state, and it was positioned in a reclined posture via single-point constraint (SPC) boundaries in the Oasys Primer for sitting in a zero-gravity seat, as shown in Figure 2. Ninety-nine springs and SPC boundaries were used to reposition the THUMS model. Points A and B in the THUMS model represent the original and target postures, respectively. A spring with a stiffness of 500 N/mm connected point A and fixed point B, and an Ls-DYNA analysis was conducted to position the THUMS. The seat was modeled with rigid slabs to eliminate any influence of materials or seat features. The crash pulse was collected from the left side of the vehicle's B-pillar during a frontal sled test at 50 km/h. The maximum acceleration of the pulse was 27.6 g, and the occupant load criterion (OLC) used for evaluating vehicle deceleration during impact was 21 g.

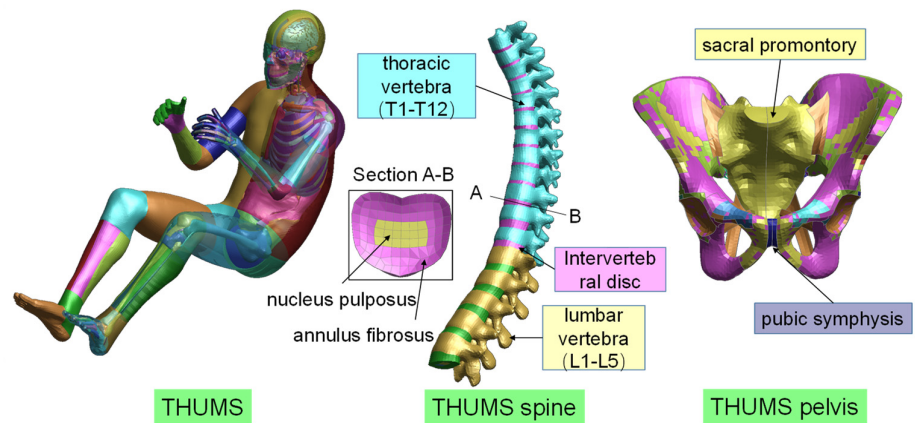


Figure 1. THUMS human biomechanical model for simulations.

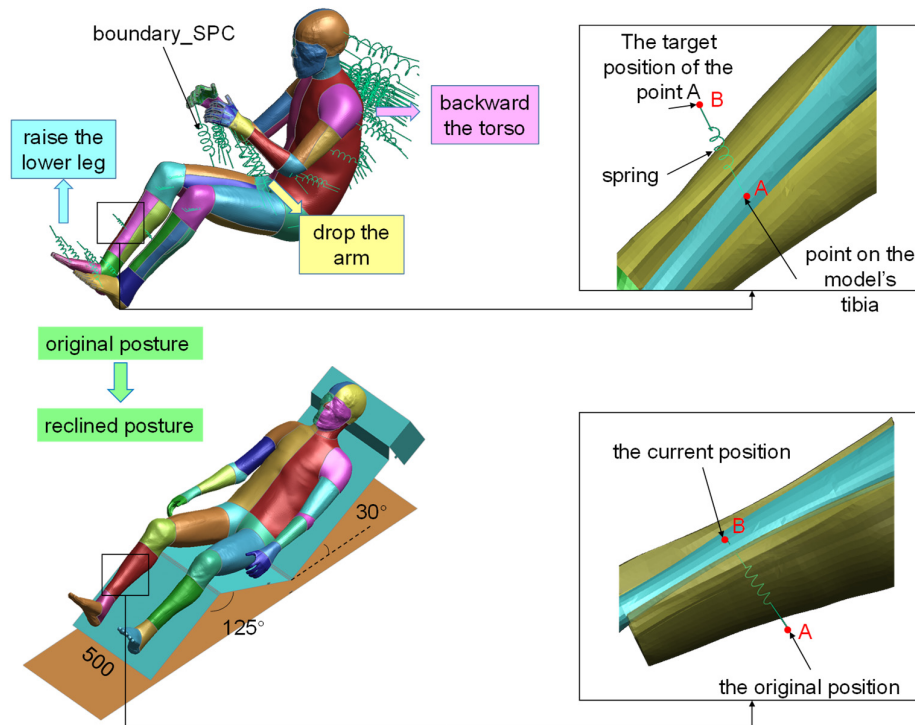


Figure 2. THUMS positioning and seat configurations.

2.2. Simulation Matrix for Different Constrained Systems

Twenty simulations were conducted to compare the injury to a reclined occupant on a normal fixed seat and a swiveling seat under a frontal sled pulse. Investigations of the effects of the constraint system, such as the effects of seatbelts, pre-tensioners, DLT, and seat movements on the injury of reclined occupants included seven types of seatbelts, two pre-tensioners, and three seat movements.

2.2.1. Seat

Three types of relative motions between the seat and vehicle floor were designed: fixed, passively swiveling, and actively swiveling seats. First, the seat was fixed to the floor. In case two, the seat was rotated counterclockwise around axis AB (Figure 3a) by the inertia of the occupant, and the relative position between axis AB and the floor was constant during the crash. The energy-absorbing structure under the seat pan was modeled using springs with different properties to investigate the effect of buffering on occupant injury, as shown in Figure 3b. In Simulation 9, for example, the seat was stationary until the spring was subjected

to a force greater than 1000 N. Subsequently, the entire seat rotated around the AB axis with the spring force maintained at 1000 N until the seat returned to the standard upright position. In Simulation 10, the collapse force of the spring in the first 40 mm was 200 N, in order to make the occupant return to the upright position quickly; later, the compressed force increased to 1000 N. In case three, the seat actively rotated 23° around axis AB for 100 ms to return to a normal configuration (no reclining) before the crash.

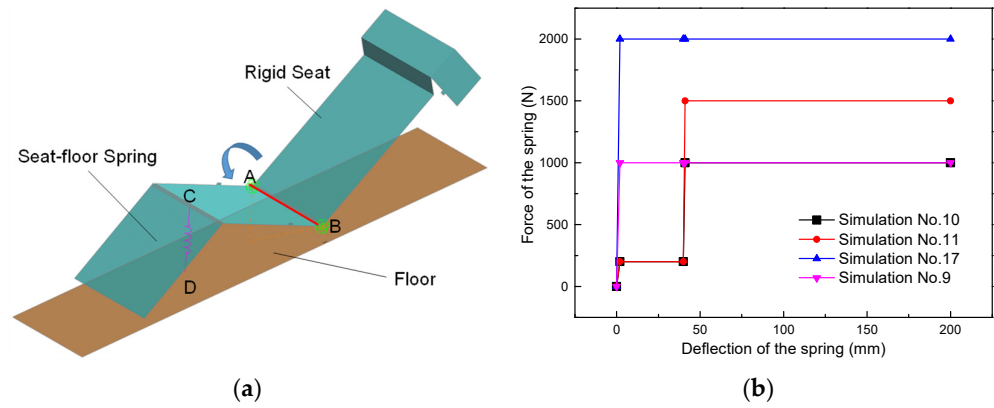


Figure 3. (a): Mechanism of the swiveling seat; (b): property of the seat floor spring.

2.2.2. Constraint System

The seatbelt form and installation points were designed for seven cases, as listed in Table 1. Case A represents a normal three-point seatbelt of which the retractor and anchor were mounted on the floor. To improve the restraint of the belt on the pelvis, Case B moved the buckle and anchor forward by 160 mm and installed the anchor on the seat pan. In Case C, the belt for the knee restraint increased. Case D consisted of a lap belt, a normal three-point seatbelt, and a knee belt, improving the upper torso restraint compared to Case C. Case E moved the retractor to the seatback, dealing with the motion of the seat relative to the floor. Case F changed the three-point thoracic belt to a four-point belt based on Case D. Case G moved the two retractors from the floor to the seatback.

Table 1. Seven belt forms for the sled simulations.

A	B	C	D	E	F	G
Three-point belt	Move forward anchor	Knee constraint	Enhanced pelvis constraint	Retractor on seatback	Four-point thorax belt	Retractor on seatback

The pretensioner, retractor PLP, and DLT were modeled using Oasys Primer. The force limit in the knee belt, lap belt, and three-point thoracic belt was 2300, 2200 and 3500 N, respectively. The four-point thoracic belt had two retractors; therefore, the force limit in each belt was 1750 N, to maintain a restraint level similar to that of the three-point belt. The pre-tensioner was activated at 9 ms and 15 ms after the crash to compare the effect of preload time on occupant movement. The DLT was realized by setting the lockup time of the slip ring. In this study, the lockup time was set to 45 ms from the beginning of the simulation by analyzing the sliding of the belt between the slip rings.

The detailed parameters of the seats and seatbelts in the 20 simulations are summarized in Table 2. The first two simulations investigated the effect of the pretensioner acting time on occupant injury. Simulations 3–8 aimed to solve the problem of submarines due to the

reclining posture by changing the anchor point, adopting PLP, DLT, and increasing the knee constraint. Simulations 9–18 tried to balance the anti-submarining and high spinal forces by allowing the seat to rotate. Simulations 19–20 rotated the seat during/before the impact to study the influence of the seat rotation mode on the injury.

Table 2. Configurations of seat and seatbelt in simulations.

Simulation No.	Pretension Time (ms)	Seatbelt Form	Seat Constraint	Seat-Pan Spring Stiffness (N) ¹	Seat Acting Time
1	15	A ²	fixed	-	-
2	9	A	fixed	-	-
3	9	B	fixed	-	-
4	9	B + PLP	fixed	-	-
5	9	B + PLP + DLT ³	fixed	-	-
6	9	C + PLP ⁴	fixed	-	-
7	9	C + PLP + DLT	fixed	-	-
8	9	D + PLP	fixed	-	-
9	9	D + PLP	passive rotation	1000	during impact
10	9	D + PLP	passive rotation	200–1000	during impact
11	9	D + PLP	passive rotation	200–1500	during impact
12	9	E + PLP	passive rotation	2000	during impact
13	9	E + PLP	passive rotation	200–2000	during impact
14	9	E + PLP	passive rotation	200–3000	during impact
15	9	F + PLP	passive rotation	500	during impact
16	9	F + PLP	passive rotation	1000	during impact
17	9	G + PLP	passive rotation	2000	during impact
18	9	G + PLP	passive rotation	4000	during impact
19	9	G + PLP	active rotation	-	during impact
20	9	G + PLP	active rotation	-	before impact

¹ The seat-pan spring stiffness represents the force generated when the spring is compressed. In this column, if there is a constant, it indicates the spring force under the entire compression. If there were two constants, they showed spring forces before and after 40 mm compression, respectively. ² A to G represent the belt forms, as shown in Table 1. ³ DLT means dynamic locking tongue. ⁴ PLP means passenger lap pretension.

2.3. Occupant Dynamics Analysis

The head injury of the occupant was assessed using the head injury criterion (*HIC*) and cumulative strain damage measure (*CSDM*) [20,21] to consider the effects of both translational and rotational acceleration. The accelerometer mounted on the head (Figure 4) recorded the head acceleration during the impact of the *HIC*, which was defined as the Formula (1). The time history of the head acceleration is represented by $a(t)$, and t_1 and t_2 are 15 ms intervals over the head acceleration curve. The *CSDM* evaluates the injury probability based on the volume of the maximal principal strain of the brain, which is greater than 0.25. The injury risk based on the *CSDM* was calculated using Equation (2). The volume proportion of brain tissue with a strain larger than 0.25 during the impact is represented by *CSDM* (0.25), and the corresponding risk of diffuse axonal injury of the occupant’s head is represented by P .

$$HIC_{15} = \max \left[\frac{1}{t_2 - t_1} \int_{t_1}^{t_2} a(t) dt \right]^{2.5} (t_2 - t_1) \tag{1}$$

$$P = \frac{1}{1 + e^{-7.86 \times CSDM(0.25) + 4.236}} \tag{2}$$

Thoracic and abdominal deflections were used to study injuries to the ribcage and visceral organs. The anteroposterior diameter of the thoracic cavity was defined as the distance from the sternum to the thoracic vertebrae. The anteroposterior diameter of the abdomen was measured on the basis of the skin around the pelvis. Cross-sections were set on all intervertebral discs of the thoracic and lumbar regions to output the axial forces and bending moments. The von Mises strains of the pelvis and femur were obtained from the results to analyze whether restraint of the lap and knee belts caused severe injury to the lower limb. The excursions of the landmarks on the left and right knees were recorded to determine the maximum forward displacement of the passenger. The relative position of pelvis and lap belt during the impact were used to illustrate the submarining which

occurred when the lap seatbelt moved over the anterior superior iliac spine (ASIS) of the occupant. The detailed measurement points are shown in Figure 4.

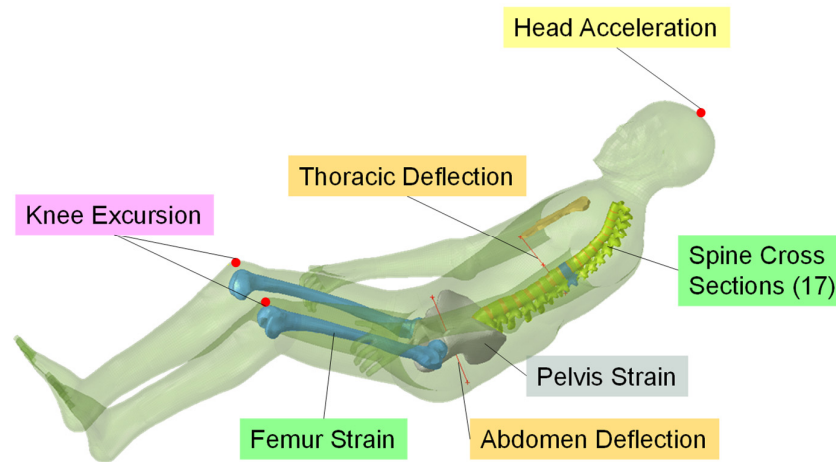


Figure 4. Measure points and output of the simulation.

3. Results

3.1. Head

The HIC and CSDM (0.25) values of the 20 simulations are plotted in Figure 5. According to the China-New Car Assessment Program (C-NCAP), occupants are at high risk of head injury when the HIC value is greater than 700. When HIC was less than 500, the head was considered safe. Hertz [22] fitted the relationship between HIC and head injury based on experimental data, and the results showed that occupants with an HIC of 500 had a head injury risk of 20%. The highest risk of diffuse axonal injury among the 20 simulations in the current study was 14.3% (Simulation 1), which was considered acceptable.

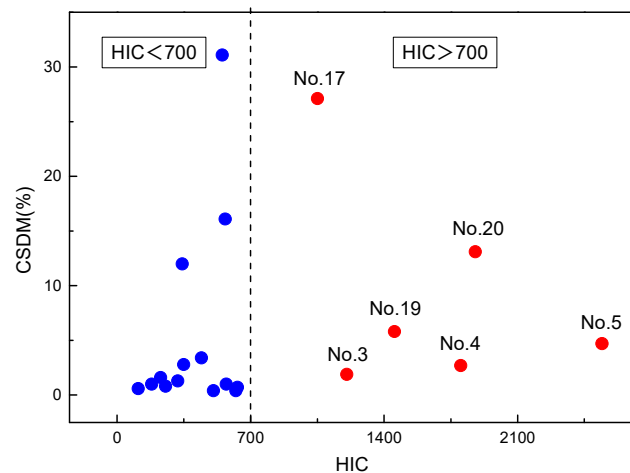


Figure 5. HIC and CSDM in the twenty simulations.

The head accelerations of the six simulations with HIC values greater than 700 are shown in Figure 6. In Simulations 3–5, the passengers were restrained with the same seatbelt, and the peak value of head acceleration occurred at about 105 ms after impact. At that time, the torso of the occupant was restricted from moving forward by the seatbelt, which caused a sudden change in head dynamics. The maximum acceleration of the head in Simulation 19 and 20 occurred at 11 ms, when the rigid headrest hit the back of the head.

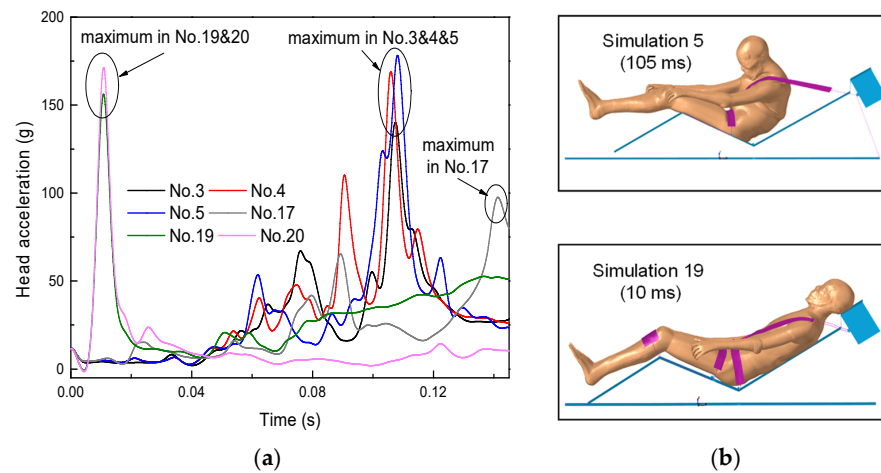


Figure 6. Head injury results: (a) head acceleration with an HIC higher than 700; (b) occupant dynamics at the peak head acceleration.

3.2. Thorax and Abdomen

The thoracic deflections in Simulations 1–14 were positive, indicating that the chest radial distance was greater than the initial (Figure 7a). When the seat was fixed on the floor, the axial compression force caused by the fixed seat pan (F2) and the occupant inertia (F1) were applied to the rib cage, resulting in a positive thoracic deflection (L1 to L2), as in Simulation 5 shown in Figure 7b. When the seat could rotate and was equipped with an energy-absorbing spring, the compression force F2 produced by the seat pan decreased, thereby theoretically reducing the anteroposterior diameter of the thoracic cavity. However, the three-point seatbelt had poor restraint on the reclined thorax, as shown in Simulation 12 (Figure 7c). The chest belt moved upward to the right rib cage during the impact, causing severe local deformation. Simulations 15–20 adopted a four-point thorax belt to optimize the restraint on the chest, such as in Simulation 19, making the thorax deflection negative and lower in absolute value compared to Simulation 1–14. The abdominal deflections in the 20 simulations ranged from 20–40 mm, and most values were approximately 28 mm.

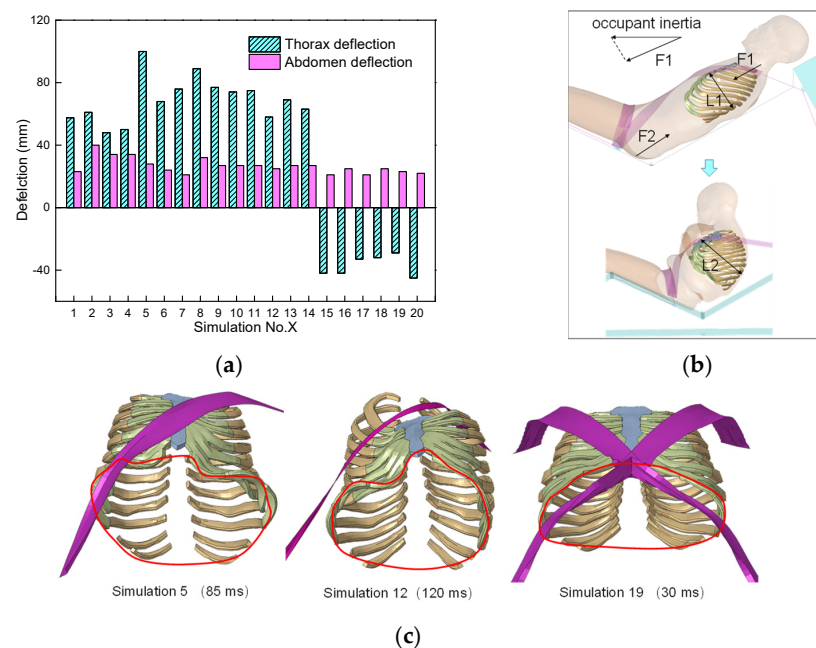


Figure 7. Response of the thorax and abdomen: (a) deflections of the occupants in the thorax and abdomen; (b) mechanism of positive thoracic deflection on a reclined occupant with a fixed seat; (c) thorax

deflections in three kinds of restraints of a three-point belt with a fixed seat, a three-point belt with a swiveling seat, and a four-point belt with a rotational seat.

3.3. Spine

The most vulnerable part of the spine during impact in reclined occupants was located at T11-L1 (from the eleventh thoracic vertebra to the first lumbar vertebra), as listed in Table 3. In Simulations 1–8, the constraints on the pelvis were promoted to reduce the submarine risk of the reclined passenger, causing the spine force to reach 5000 N, which is higher than the spine injury threshold of 4800 N proposed by Maiman et al. [23]. The maximum spine force in Simulation 8 was lower than that in Simulation 7; this is because the additional belt in Simulation 8 increases the restraint area on the occupant, causing the impact load to be applied more evenly across the lumbar spine.

Table 3. Spine injury summary.

Simulation No.	Maximum Axial Force			Maximum Moment		
	Value (N)	Location	Time (ms)	Value (N·m)	Location	Time (ms)
1	2574.2	T12-L1	67	30.4	T12-L1	93
2	2969.8	T11-T12	94	34.1	T12-L1	94
3	3833.9	T11-T12	87	34.1	T12-L1	92
4	4043.2	T11-T12	88	34.5	T12-L1	90
5	5061.9	T12-L1	90	44.2	T12-L1	87
6	5022.3	T11-T12	79	39.4	T12-L1	83
7	5359.3	T12-L1	86	40.9	T12-L1	83
8	4807.7	T11-T12	93	38	T12-L1	91
9	4003.4	T11-T12	90	33.3	T12-L1	90
10	3863.2	T11-T12	89	32.2	T12-L1	86
11	3924.7	T11-T12	89	32.5	T12-L1	87
12	3683.5	L1-L2	104	25.3	T12-L1	101
13	4375.5	T12-L1	103	30.1	T12-L1	101
14	4179.1	T12-L1	104	30.1	T12-L1	102
15	2756.9	T12-L1	93	27.2	T12-L1	95
16	2849.2	T11-T12	94	28.3	T12-L1	93
17	1787.2	L2-L3	64	16.8	L2-L3	159
18	1870.9	L2-L3	64	13.7	T12-L1	122
19	2140.2	L1-L2	110	20.7	T12-L1	110
20	2142	T12-L1	162	22	T12-L1	184

Simulations 9–14 allowed the seat to rotate around the pan-back axle, and the upper torso was restrained using a three-point belt. In these simulations, the maximum axial force in the spine was approximately 4000 N, which is a reduction of 1000 N compared with those with a fixed seat. When the retractor was fixed on the floor (Simulations 9–11), the spinal injury was insensitive to the spring stiffness, because the thorax belt connected to the floor limited the rotation of the seat. One hypothesis is that a lower initial spring stiffness would allow the occupant to return to an upright posture earlier, and reduce the risk of spinal injury. However, the results of Simulations 12–14 showed that a constant stiffness spring of 2000 N contributes to a lower spine force. This could be attributed to the fact that the large initial rotational stiffness of the seat pan helped restrain the occupants and absorb impact energy.

Simulations 15–18 adopted a four-point thoracic belt to promote constraint on the upper torso, significantly reducing the axial force and bending moment of the spine. In Simulations 15 and 16, the retractors were mounted on the floor, and the maximum spine force was approximately 2800 N which was almost half that in Simulation 7. Simulations 17 and 18 moved the retractor to the seatback, and the peak spine force was 1800 N. The spring stiffness in Simulation 18 was twice that in Simulation 17, whereas the spinal injury in the two simulations showed little difference. The seat in Simulations 19 and 20 ro-

tated actively during and before impact. The maximum spinal force in the two simulations was approximately 2140 N which was 300 N higher than that in the passive seat.

The maximum von Mises strains from T10 to L3 in the 20 simulations during the impact are shown in Figure 8. Overall, only Simulations 17, 18, and 20 had a maximum spinal strain less than 0.03, which is considered the injury threshold of the vertebra [24,25]. In Simulations 1 and 2, the serving submarining of the occupant causes the maximum strain to reach 0.1 and occur in the transverse process. Enhanced pelvic restraint aggravated the curvature of the upper torso, and the maximum spinal strain shifted to the 12th vertebra. As shown in Figure 8c–h, the peak strain reached approximately 0.15, which is five times higher than the injury threshold of the vertebra. Figure 8i–p showed the injury results of the occupant with the swivel seat, where the maximum strain of the vertebra decreased to approximately 0.08. As shown in Figure 8q,r, the peak strain is approximately 0.006, which is lower than the injury threshold. In both cases, the reclined occupant was placed on the swiveling seat with the retractor integrated on the seatback, and the PLP, knee constraint, and four-point belt were adopted.

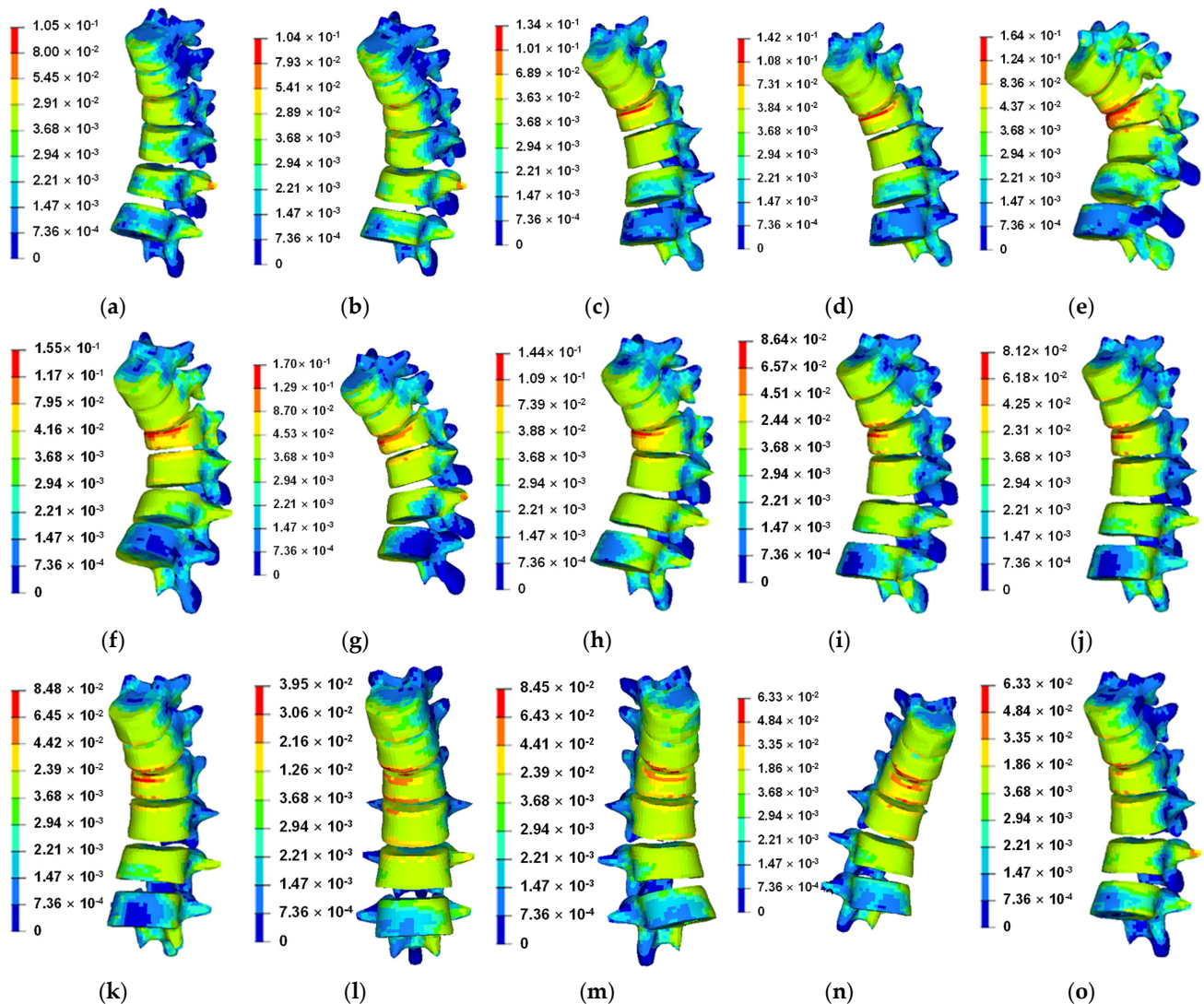


Figure 8. Cont.

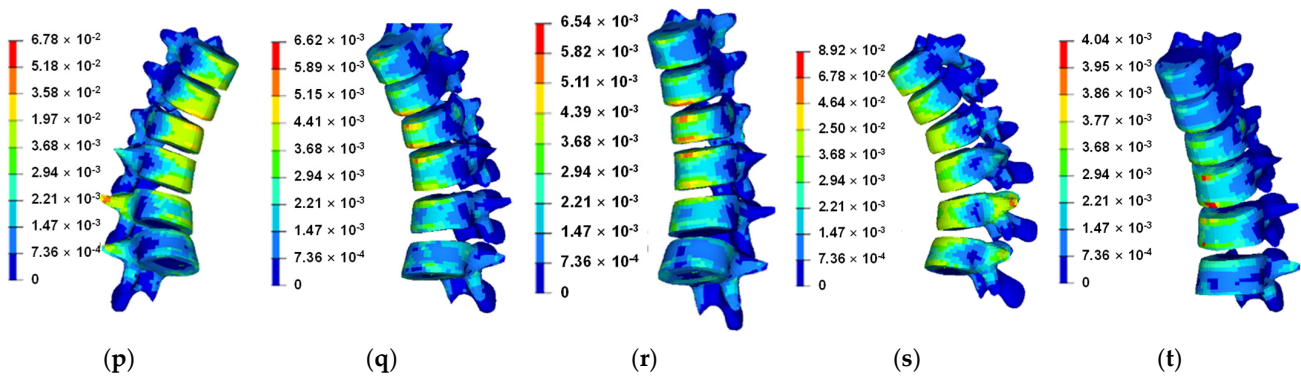


Figure 8. The maximum strain from T10 to L3 during impact: (a–t) represent the simulation results from 1 to 20.

Figure 9 plots the spine morphology during impact in Simulations 7 and 18. The various colored lines depict the centerlines of the spines at different times, and the green outline shows the spine with the maximum axial force. In Simulation 7, the shape of the spine changed slightly during the previous 45 ms. After 45 ms, the rigid seat pan and seatbelt prevented the pelvis from moving forward, whereas the upper torso continued to move inertially, causing the lumbar spine to experience serious axial compression. Additionally, the poor restraint of the three-point belt in reclined passengers exacerbated injury to the lumbar spine.

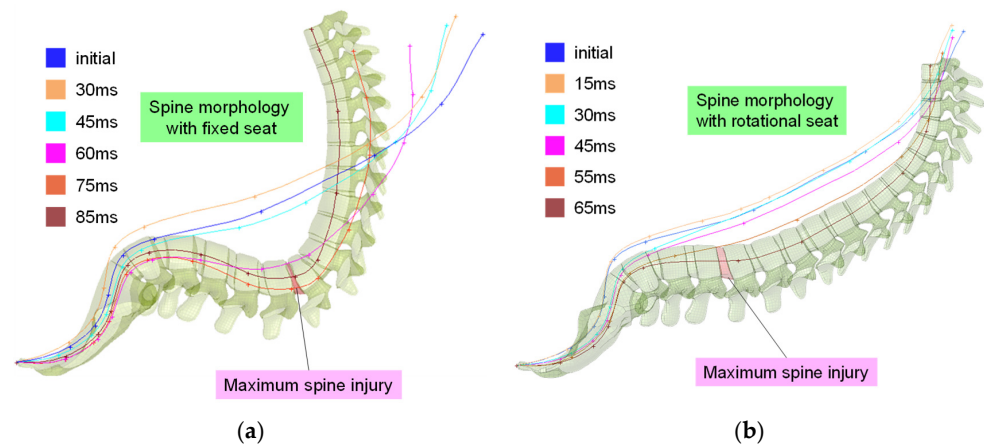


Figure 9. Spine morphology during the impact (a) with fixed seat (Simulation 7); and (b) with rotational seat (Simulation 18).

As shown in Figure 9b, the pelvic angle did not decrease significantly, although the seat could rotate during the impact, which meant that the occupant was also subjected to a crash with the original reclined posture. In contrast to the fixed seat in Simulation 7, the rotated seat in Simulation 18 allowed the occupant to move forward (see the knee excursion in Table 3) relative to the floor, providing a larger space for the restraint system to absorb impact energy. The rotating seat also lowers the height of the pelvis, thereby avoiding severe local deformation of the lumbar spine.

3.4. Pelvis and Lower Limbs

Figure 10 showed the submarining results of three typical simulations during the impact in Simulation 1; the reclined passenger was restrained by a normal three-point seatbelt, and the lap belt was completely moved to the abdomen during the impact, as shown in Figure 10. Simulations 2–4 optimized the occupant restraint; however, submarining still occurred. In Simulations 5–20, the lap belt restrained well, and no submarining occurred.

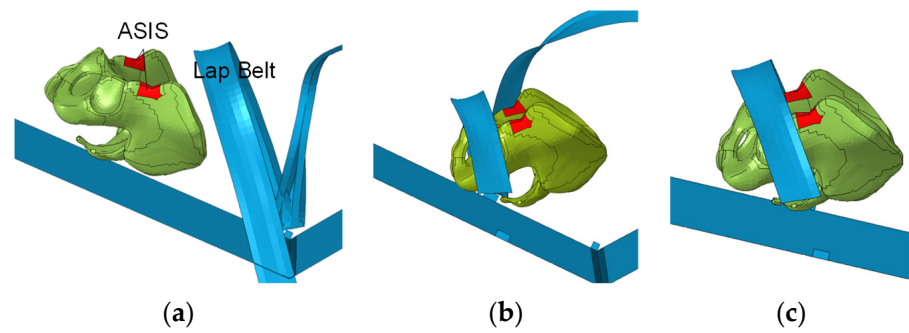


Figure 10. The position of pelvis and lap belt in (a) Simulation 1 at 120 ms; (b) Simulation 5 at 80 ms; and (c) Simulation 18 at 105 ms.

A large pelvic constraint force causes pelvic injury, as assessed by the effective plastic strain of the cortical bone, as shown in Table 4. In the simulations with a swiveling seat, the maximum strain of the pelvis was less than the injury criterion of 2.57%, except for Simulation 13, in which the seat-pan spring might not have been able to absorb sufficient impact energy. When the occupant was on a fixed seat, the maximum strain of the pelvis ranged from 2.2 to 5.6, causing high injury risk. The risk of lower limb injury was also assessed. The maximum strain in the femur was less than the injury criterion of 2.14% in all simulations, indicating that the knee restraint did not cause additional damage to the lower limbs.

Table 4. Pelvic injury summary.

Simulation No.	1	2	3	4	5	6	7	8	9	10
Pelvis Maximum Stain (%)	4.6	2.6	3.8	3.8	5.6	3.4	3	2.2	1.9	1.9
Femur Maximum Stain (%)	0.38	0.35	0.54	0.59	1.3	1.2	1.1	0.5	0.4	0.4
Knee Excursion (mm)	273	252	260	251	154	116	95	113.2	162	185
Simulation No.	11	12	13	14	15	16	17	18	19	20
Pelvis Maximum Stain (%)	2	2.4	3	2.4	2.1	1.9	2.7	1.9	2	2.7
Femur Maximum Stain (%)	0.4	0.8	0.7	0.7	0.5	0.5	0.8	0.5	0.5	0.6
Knee Excursion (mm)	185	265	278	272	182	180	300	245	270	313.1

Figure 11 shows the motion trajectories of the knees in the sagittal (x–z) plane for the 20 simulations. In Figure 11a, the knee excursions of occupants with a fixed seat were above the initial position of the knee during the impact. This makes the occupant’s posture appear V-shaped, increasing the curvature of the spine and exacerbating the associated damage. Figure 11b depicts the knee trajectories of occupants with swiveling seats and three-point normal thoracic belts. In these simulations, the knee moved below its initial position in the z direction. When the retractors were integrated on the seatback (Simulations 12, 13 and 14), the maximum displacements of the knee in both the X and Z directions were approximately 100 mm larger than those with fixed retractors on the floor. Figure 11c shows the results of Simulations 15–20, in which the reclined occupants were placed on the swiveling seat and restrained with a four-point thorax belt. The maximum displacements in Simulations 17 and 20 were 300 mm.

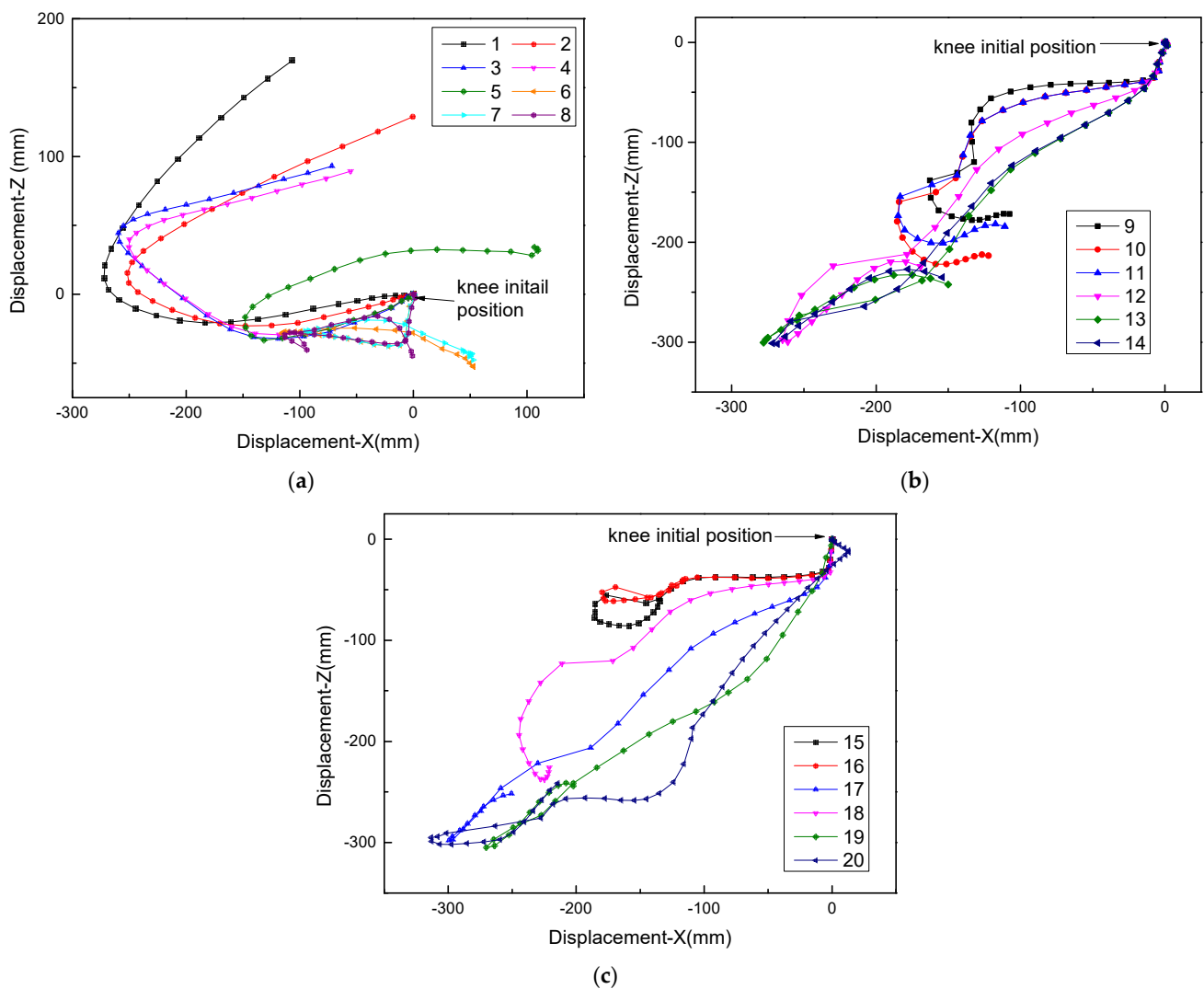


Figure 11. The motion trajectories of knees in the sagittal (x-z) plane: (a) Simulations 1–8; (b) Simulations 9–14; and (c) Simulations 15–20.

4. Discussion

The reclined sitting position becomes a general posture during driving, and the current restraint system is not able to protect the occupant. This study proposed a swiveling seat, and conducted 20 simulations to investigate the protection of reclined occupants. The results contribute to promoting the safety of out-of-position occupants in automobile design.

In simulation 1, severe submarining accompanied by abdominal injury occurred when a reclined passenger was equipped with a normal three-point seatbelt. The first challenge in developing a novel restraint system for reclined people is solving the submarine problem. The anchor pretensioner, DLT, and belt angle were used in Simulation 5, and submarining was successfully avoided. In this simulation, the pelvis was subjected to a heavy load from the seatbelt, causing a maximum strain of 5.6%, which is higher than the pelvic injury strain of 2.14%. The maximum strain of the pelvis in Simulation 6–8 was decreased to approximately 1% by adopting an extra knee belt and a lap belt. This showed that a large contact area between the restraint system and the occupant could effectively reduce the risk of injury to the pelvis. Some researchers used knee bolsters to increase the contact area and relieve the load applied to the pelvis [26,27]. The properties and initial position of the knee bolster need to be considered because the large occupant-to-knee bolster distance was not able to reduce the submarining risk, and a hard knee bolster would lead to lower limb injury [18].

Extra belts eliminate the concentrated load on the pelvis; however, the problems of high lumbar compression forces and bending moments remain unsolved, as shown in Table 3. The GHBM numerical study simulated by Boyle et al. [28] and the PMHS experiments conducted by Richardson et al. [29] showed a similar phenomenon in that the lumbar spine of the reclined occupant was loaded in compression and bending during the crash. The rotated seat in this study aims to make the reclined occupant upright during frontal impact to mitigate injury. However, the simulation results of the current study showed that the pelvic angle changed little during the rotational movement of the seat, which can be attributed to the flexibility of the lumbar spine in the biomechanical model. Study conducted by Östh et al. [30] also showed that the pelvis of reclined human body model did not return upright under seat-back repositioning. Therefore, an upright pelvis was not considered necessary to minimize the injury of the reclined occupants because the lumbar force in Simulation 18 (with a high pelvis angle during the impact) was 1870 N, which was lower than the spine injury threshold.

In this study, one of the significant factors affecting the low lumbar force in Simulations 17–20 was that the swivel seat allowed passengers a greater forward movement relative to the floor. A large passenger displacement can allow the restraint system to play its full role, and reduce the impact energy that must be absorbed by the occupant and the resultant injury risk. Simulation 17 had the minimum spine force of 1787 N among the 20 simulations, and its knee excursion was 300 mm, which was larger than that of the others. The knee excursion in Simulation 7 was 95 mm, and the axial force in the first lumbar region reached 5359 N, which was the maximum value among the 20 cases. Additionally, the swivel seat in this study lowered the center of gravity of the pelvis during impact, reducing the curvature of the spine and the associated injury risk [31], as shown in Figure 9. In methods wherein the reclined occupant returns to a normal sitting configuration by raising their upper torso, the safety system needs to provide the occupant with an additional upward force, possibly increasing the axial force acting on the spine. In this study, the center of gravity of the lower body decreased during the collision, which helped reduce the curvature of the spine and relieve the spinal force.

The seat-integrated belt system could provide better protection for occupants with diverse sitting configurations because the retractor, anchor, and slip rings could adapt to seat movement [32]. For the reclined occupant, the protection provided by the normal three-point safety belt was unsatisfactory, owing to its poor restraining properties. Swivel seats were used in Simulation 12 and Simulation 17, with the first one adopting a three-point belt and the second adopting a four-point belt. The results showed that the lumbar force in Simulation 12 was 3683 N, which was twice as high as that in Simulation 17. This indicates that improving the restraint performance can significantly reduce occupant injuries. New safety systems such as seats or other restraint system [33,34] should not cause additional injury to passengers before a crash. Simulation 20 with an active rotational seat in this study caused a head acceleration of more than 350 g at 11 ms after impact, because the rotational seatback hit the head. Thus, the speed and force of execution need to be studied further.

The limitations of this study were as follows. First, the protective performance of the swiveling seat for a reclined occupant was evaluated using a frontal impact sled. Further assessments of seats in complex traffic scenarios should be considered. Second, the properties of the energy-absorbing structure under the seat pan were designed for a 50th-percentile human model. The performance of the swiveling seat for 5th- or 95th-percentile humans could be further studied.

5. Conclusions

Safety systems for high-tilt reclined occupants face the challenges of submarining and large lumbar forces during a crash. The current study proposes a swivel seat that can return to the upright configuration based on the occupant's inertia during impact. Twenty simulations based on a human biomechanical model of the frontal sled were conducted to investigate the effectiveness of the seat. The results showed that the swiveling seat with

a four-point belt successfully prevented the submarining and created a lumbar force of approximately 1800 N within the injury threshold. Meanwhile, the swiveling seat did not contribute to additional injuries to the head, thorax, abdomen, pelvis, or knee of the occupants. The findings of this study have great potential for protecting reclined occupant in intelligent driving scenarios.

Author Contributions: Conceptualization, F.T. and Y.W.; methodology, J.C., Y.W. and F.T.; software, F.T., F.L. and Y.W.; validation, F.T. and Q.J.; formal analysis, F.L. and J.C.; investigation, Q.J. and Y.W.; resources, Y.W. and F.L.; data curation, Q.J.; writing—original draft preparation, F.T. and Y.W.; writing—review and editing, F.L. and J.C.; visualization, J.C.; supervision, Q.J.; project administration, F.T.; funding acquisition, F.T. and F.L. All authors have read and agreed to the published version of the manuscript.

Funding: F.T. acknowledges support from the postdoctoral research project of Guangzhou. F.L. acknowledges the support from National Natural Science Foundation of China, grant numbers [52175267].

Institutional Review Board Statement: Not applicable.

Informed Consent Statement: Not applicable.

Data Availability Statement: The data presented in this study are available on request from the corresponding author. The data are not publicly available due to privacy.

Conflicts of Interest: The authors declare no conflicts of interest.

References

1. Sun, X.; Cao, S.; Tang, P. Shaping driver-vehicle interaction in autonomous vehicles—How the new in-vehicle systems match the human needs. *Appl. Ergon.* **2021**, *21*, S66–S71. [\[CrossRef\]](#)
2. Nie, B.; Gan, S.; Chen, W.; Zhou, Q. Seating preferences in highly automated vehicles and occupant safety awareness: A national survey of Chinese perceptions. *Traffic Inj. Prev.* **2020**, *21*, 247–253. [\[CrossRef\]](#)
3. Timothy, L.M.; Gerald, S.P.; Greg, S.; Matthew, B.P. Crash safety concerns for out-of-position occupant postures: A look toward safety in highly automated vehicles. *Traffic Inj. Prev.* **2018**, *19*, 582–587.
4. Östling, M.; Annika, L. Occupant activities and sitting positions in automated vehicles in China and Sweden. In Proceedings of the Enhanced Safety Vehicles (ESV), Eindhoven, The Netherlands, 22 June 2019.
5. Jorlöv, S.; Bohman, K.; Annika, L. Seating positions and activities in highly automated cars—A qualitative study of future automated driving scenarios. In Proceedings of the IRCOBI Conference, Antwerp, Belgium, 13–15 September 2017.
6. Rehm, C.G.; Goldman, R.K. Seat belt and car seat in a reclined position—a dangerous combination. *J. Trauma* **2021**, *51*, 1189–1191. [\[CrossRef\]](#)
7. Schaefer, L.C.; Junge, M.; Voros, I.; Koçaslan, K.; Becker, U. Odds ratios for reclined seating positions in real-world crashes. *Accid. Anal. Prev.* **2021**, *161*, 106357. [\[CrossRef\]](#)
8. Talimian, A.; Vychytil, J. Numerical study of frontal collision effects on an occupant's safety, in autonomous vehicles, with non-standard seating configurations. *Acta. Polytech. Hung.* **2021**, *18*, 127–140. [\[CrossRef\]](#)
9. Leledakis, A.; Osth, J.; Davidsson, J.; Jakobsson, L. The influence of car passengers' sitting postures in intersection crashes. *Accid. Anal. Prev.* **2021**, *157*, 106170. [\[CrossRef\]](#)
10. Mroz, K.; Östling, M.; Richardson, R.; Kerrigan, J.; Forman, J.; Gepner, B.; Nils, L.B.P. Effect of seat and seat belt characteristics on the lumbar spine and pelvis loading of the SAFER human body model in reclined postures. In Proceedings of the IRCOBI Conference, Munich, Germany, 1 September 2020.
11. Wu, H.; Hou, H.; Shen, M.; Yang, K.H.; Jin, X. Occupant kinematics and biomechanics during frontal collision in autonomous vehicles—can rotatable seat provides additional protection. *Comput. Methods Biomec.* **2019**, *23*, 191–200. [\[CrossRef\]](#)
12. Gepner, B.D.; Draper, D.; Mroz, K.; Richardson, R.; Ostling, M.; Pipkorn, B.; Forman, J.L.; Kerrigan, J.R. Comparison of human body models in frontal crashes with reclined seatback. In Proceedings of the IRCOBI Conference, Florence, Italy, 11–13 September 2019.
13. Grebonval, C.; Trosseille, X.; Petit, P.; Wang, X.; Beillas, P. Effects of seat pan and pelvis angles on the occupant response in a reclined position during a frontal crash. *PLoS ONE* **2021**, *16*, e0257292. [\[CrossRef\]](#)
14. Rawska, K.; Gepner, B.; Moreau, D.; Kerrigan, J.R. Submarining sensitivity across varied seat configurations in autonomous driving system environment. *Traffic Inj. Prev.* **2022**, *21*, S1–S6. [\[CrossRef\]](#)
15. Richardson, R.; Donlon, J.P.; Chastain, K.; Shaw, G.; Forman, J. Test methodology for evaluating the reclined seating environment with human surrogates. In Proceedings of the Enhanced Safety Vehicles (ESV), Eindhoven, The Netherlands, 22 June 2019.
16. Richardson, R.; Jayathirtha, M.; Chastain, K.; Donlon, J.P.; Forman, J.; Gepner, B.; Östling, M.; Mroz, K.; Shaw, G.; Pipkorn, B.; et al. Thoracolumbar spine kinematics and injuries in frontal impacts with reclined occupants. *Traffic Inj. Prev.* **2020**, *21*, S66–S71. [\[CrossRef\]](#)

17. Matsushita, T.; Saito, H.; Sunnevång, C.; Östling, M.; Vishwanatha, A.; Tabhane, A. Evaluation of the protective performance of a novel restraint system for highly automated vehicles. In Proceedings of the Enhanced Safety Vehicles (ESV), Eindhoven, The Netherlands, 22 June 2019.
18. Rawska, K.; Gepner, B.; Kulkarni, S.; Chastain, K.; Zhu, J.; Richardson, R.; Perez, R.D.; Forman, J.; Kerrigan, J.R. Submarining sensitivity across varied anthropometry in an autonomous driving system environment. *Traffic Inj. Prev.* **2019**, *20*, S123–S127. [[CrossRef](#)]
19. Kang, M.; Kim, H.; Cho, Y.; Kim, S.; Lim, D. Occupant safety effectiveness of proactive safety seat in autonomous emergency braking. *Sci. Rep.* **2022**, *12*, 5727. [[CrossRef](#)]
20. Kleiven, S. Predictors for traumatic brain injuries evaluated through accident reconstructions. *Stapp Car Crash J.* **2007**, *51*, 81–114.
21. Takhounts, E.G.; Eppinger, R.H.; Campbell, J.Q.; Tannous, R.E.; Power, E.D.; Shook, L.S. On the development of the SIMon finite element head model. *Stapp Car Crash J.* **2003**, *47*, 107–133.
22. Hertz, E. A note on the head injury criterion (HIC) as a predictor of the risk of skull fracture. *Publ. Assoc. Adv. Automot. Med.* **1993**, *37*, 303–312.
23. Maiman, D.J.; Sances, A.J.; Myklebust, J.B.; Larson, S.J.; Houterman, C.; Chilbert, M.; El-Ghatit, A.Z. Compression injuries of the cervical spine: A biomechanical analysis. *Neurosurgery* **1983**, *13*, 254–260. [[CrossRef](#)]
24. Burstein, A.H.; Reilly, D.T.; Martens, M. Aging of bone tissue: Mechanical properties. *J. Bone Jt.* **1976**, *58*, 82–86. [[CrossRef](#)]
25. McCalden, R.W.; McGeough, J.A.; Barker, M.B.; Court-Brown, C.M. Age-related changes in the tensile properties of cortical bone. *J. Bone Jt.* **1993**, *75*, 1193–1205. [[CrossRef](#)]
26. Ji, P.; Huang, Y.; Zhou, Q. Mechanisms of using knee bolster to control kinematical motion of occupant in reclined posture for lowering injury risk. *Int. J. Crashworthiness* **2017**, *22*, 415–424. [[CrossRef](#)]
27. Dissanaik, S.; Kaufman, R.; Mack, C.D.; Mock, C.; Bulger, E. The effect of reclined seats on mortality in motor vehicle collisions. *J. Trauma* **2008**, *64*, 614–619. [[CrossRef](#)]
28. Boyle, K.J.; Reed, M.P.; Zaseck, L.W.; Hu, J. A human modelling study on occupant kinematics in highly reclined seats during frontal crashes. In Proceedings of the IRCOBI Conference, Florence, Italy, 11–13 September 2019.
29. Richardson, R.; Donlon, J.P.; Jayathirtha, M.; Forman, J.L.; Shaw, G.; Gepner, B.; Kerrigan, J.R. Kinematic and injury response of reclined PMHS in frontal impact. *Stapp Car Crash J.* **2020**, *64*, 83–153.
30. Östh, J.; Bohman, K.; Jakobsson, L. Evaluation of kinematics and restraint interaction when repositioning a driver from a reclined to an upright position prior to frontal impact using active human body model simulations. In Proceedings of the IRCOBI Conference, Munich, Germany, 1 September 2020.
31. Reed, M.P.; Ebert, S.M.; Jones, M.L.H. Posture and belt fit in reclined passenger seats. *Traffic Inj. Prev.* **2019**, *20*, S38–S42. [[CrossRef](#)]
32. Thorbole, C.K. Dangers of seatback reclined in a moving vehicle how seatback recline increases the injury severity and shifts injury pattern. In Proceedings of the IMECE Conference, Houston, TX, USA, 13–19 November 2015.
33. Ngo, A.V.; Becker, J.; Thirunavukkarasu, D.; Urban, P.; Koetniyom, S.; Carmai, J. Investigation of occupant kinematics and injury risk in a reclined and rearward-facing seat under various frontal crash velocities. *J. Saf. Res.* **2021**, *79*, 26–37. [[CrossRef](#)]
34. Jin, X.; Hou, H.; Shen, M.; Wu, H.; Yang, K.H. Occupant kinematics and biomechanics with rotatable seat in autonomous vehicle collision—A preliminary concept and strategy. In Proceedings of the IRCOBI Conference, Athens, Greece, 12–14 September 2018.

Disclaimer/Publisher’s Note: The statements, opinions and data contained in all publications are solely those of the individual author(s) and contributor(s) and not of MDPI and/or the editor(s). MDPI and/or the editor(s) disclaim responsibility for any injury to people or property resulting from any ideas, methods, instructions or products referred to in the content.